

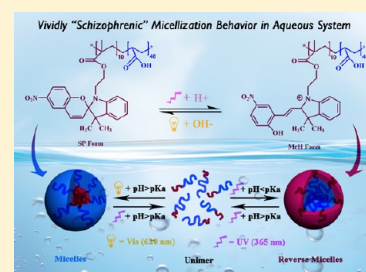
A Light and pH Dual-Stimuli-Responsive Block Copolymer Synthesized by Copper(0)-Mediated Living Radical Polymerization: Solvatochromic, Isomerization, and “Schizophrenic” Behaviors

Yin-Ning Zhou, Qing Zhang, and Zheng-Hong Luo*

Department of Chemical Engineering, School of Chemistry and Chemical Engineering, Shanghai Jiao Tong University, Shanghai 200240, P. R. China

Supporting Information

ABSTRACT: A “schizophrenic” block copolymer (poly[1'-(2-methacryloxyethyl)-3',3'-dimethyl-6-nitrospiro-(2*H*-1-benzopyran-2,2'-indoline)]-*b*-poly(acrylic acid) (PSPMA-*b*-PAA)) was synthesized by sequential copper(0)-mediated living radical polymerization (Cu(0)-mediated LRP) at 30 °C in an oxygen-tolerant system followed by hydrolysis of the resulting polymer. The solvatochromic behaviors of the PSPMA₁₀-*b*-poly(*t*-butyl acrylate)₄₀ (PSPMA₁₀-*b*-PtBA₄₀) and PSPMA₁₀-*b*-PAA₄₀ block copolymers in organic solvents were investigated by UV–vis spectroscopy. The PSPMA₁₀-*b*-PtBA₄₀ stabilizes the nonpolar photoisomer and is not sensitive to the polarity of the solvent, while the PSPMA₁₀-*b*-PAA₄₀ stabilizes the planar zwitterionic form without irradiation. Furthermore, light-induced isomerization of spiroopyran (Sp) moieties from Sp to merocyanine (Mc) was demonstrated. Finally, the “schizophrenic” micellization behavior of as-prepared copolymer in aqueous solution regulated by light and pH stimuli was vividly demonstrated, and the reversibility of micellization processes performed in this study was also examined. The large compound micelles can bring out a gradually extended and even transformed conformation with increasing deprotonation degree at pH > p*K*_a.



INTRODUCTION

The self-assembly of stimuli-responsive polymer materials has drawn increasing attention in recent years.^{1–4} Among a great variety of amphiphilic block copolymers, some amusing ones can inversely transform themselves into double hydrophilic block copolymers (DHBCs) induced by adequate external stimuli, such as pH,^{5–10} temperature,^{10–13} salt concentration,^{5,6,13–15} and light irradiation.^{15–17} Such amphiphilic block copolymers have first been named as “schizophrenic” copolymers by Armes et al.^{18,19} Because of their stimuli-tunable assembly behaviors, such “smart” switchable assembly of block copolymers has been investigated in various fields, for instance, drug delivery and controlled release,^{20–22} soft template,²³ nanoreactors,^{24,25} etc.

Multifarious external stimuli can be used to regulate block copolymer assembly. Among them, light irradiation is an attractive one attributing to its facile operation and rapid responsiveness.^{26,27} By using the merit of light, the release of encapsulated substances can be triggered at a specific time and location.²⁸ As one of the most well-known classes of organic photochromic compound, nonpolar and hydrophobic spiroopyran (Sp) can be isomerized to polar, hydrophilic, zwitterionic merocyanine (Mc) upon UV light irradiation and revert to Sp form responding to visible-light irradiation.²⁹ In an acidic aqueous solution, almost all chromophores (Sp) are of the protonated merocyanine form (McH) responding to UV irradiation; meanwhile, a few of residue Sp moieties also experience the competitive process of protonation leading to form the positively charged Sp form (SpH). Reversibly, visible-light irradiation and the addition of base result in effective

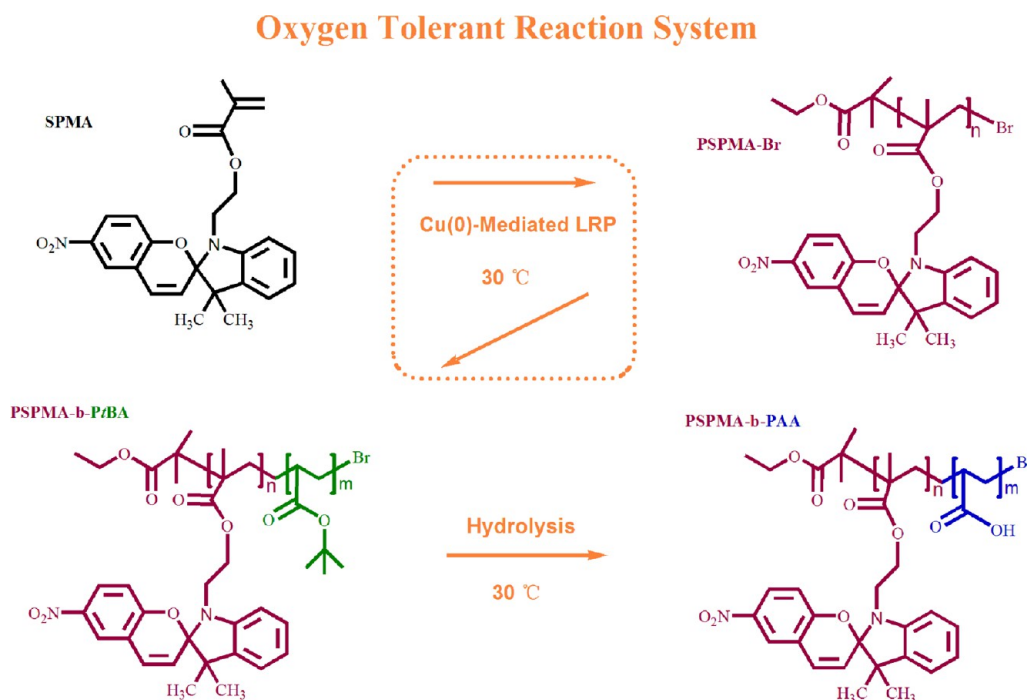
isomerization of McH into Sp. Because of these novel characteristics, the photochromic copolymers containing spiroopyran units have many potential applications,^{30–43} such as the reversible controlled release of hydrophobic dye,^{12,34,38} biological diagnosis, imaging, and detection,³⁹ colorimetric detector,^{40–42} molecular probe, etc.⁴³ In addition, acrylic acid (AA) is a typical pH-responsive monomer. Polymer chains (PAA) adopt a compact structure in aqueous solution due to protonation of carboxylate groups at pH < p*K*_a and exhibit a fully stretched conformation due to the electrostatic repulsion between –COO[–] groups generated by deprotonation of carboxyls at pH > p*K*_a.^{44–46}

Copper(0)-mediated living radical polymerization (Cu(0)-mediated LRP) is designated as single-electron transfer living radical polymerization (SET-LRP) by Percec et al.^{47,48} and termed as supplemental activator and reducing agent for atom transfer radical polymerization (SARA ATRP) by Matyjaszewski et al.^{49,50} distinguished by the role of Cu(0). Despite the undefined mechanism, it is attractive to utilize Cu(0) powder as the catalyst because Cu(0) is inexpensive and easier to be coped with than Cu(I) and Cu(II) complexes. Moreover, previous studies showed that Cu(0)-mediated LRP of acrylate monomers can be easily performed in an oxygen-tolerant system at ambient temperature by the addition of reducing agents.^{51,52}

Received: August 2, 2013

Revised: January 9, 2014

Published: January 28, 2014

Scheme 1. Synthetic Route of the PSPMA-*b*-PAA Diblock Copolymer via Sequential Cu(0)-Mediated LRP and Hydrolysis Reaction

In this work, the synthesis of “schizophrenic” block copolymers, PSPMA-*b*-PAA, was achieved via the sequential Cu(0)-mediated LRP at 30 °C in an oxygen-tolerant system followed by hydrolysis of the resulting polymers. The synthetic strategy for this light and pH dual-responsive copolymer is illustrated in Scheme 1. Moreover, the solvatochromic and light isomerization behaviors of the PSPMA₁₀-*b*-PtBA₄₀ and PSPMA₁₀-*b*-PAA₄₀ copolymers in organic solvents were investigated by UV–vis spectroscopy. Finally, we vividly demonstrated the reversible transition capability of the as-prepared copolymer between the hydrophilic and hydrophobic states (i.e., the “schizophrenic” micellization behaviors) under the regulation of light and pH stimuli.

EXPERIMENTAL SECTION

Materials. *tert*-Butyl acrylate (tBA, 99%, Sinopharm Chemical Reagent Co., Ltd. (SCRC)) was rinsed with an aqueous NaOH solution (5 wt %) to remove inhibitor, dried with MgSO₄ overnight, and distilled before use. Ethyl 2-bromoisobutyrate (Eib-Br, 98%), hexamethylated tris(2-aminoethyl)amine (Me₆TREN, 99%), and hydrazine monohydrate (N₂H₄·H₂O, 98%) were obtained from Alfa Aesar. Copper powder (75 μm, 99%) was purchased from Sigma-Aldrich. Trifluoroacetic acid (TFA, 99%) was used as received from SCRC. Toluene, chloroform, tetrahydrofuran (THF), dimethyl sulfoxide (DMSO), and dichloromethane (DCM) were obtained from SCRC and used without further purification. 1'-(2-Methacryloxyethyl)-3',3'-dimethyl-6-nitrospiro-(2*H*-1-benzopyran-2,2'-indoline) (SPMA) was synthesized through an esterification reaction according to previously reported work^{36,54} (see Supporting Information for details).

Synthesis of Macroinitiator PSPMA-Br via Cu(0)-Mediated LRP. The experiment was carried out at [M]:[I]:[C]:[L]:[R] = 15:1:0.25:0.25:0.25. Solvent (DMSO, 8 mL), SPMA (M, 1.26g, 3 mmol), catalyst (C, copper powder, 3.2 mg, 0.05 mmol), and hydrazine hydrate (R, 2.4 μL, 0.05 mmol) were added to a dried flask. The reaction mixture was stirred for 15 min in a water bath with a thermostat at 30 ± 0.1 °C after being degassed and full filled with nitrogen. And then, ligand (L, Me₆TREN, 12.8 μL, 0.05 mmol) and initiator (I, Eib-Br, 29.3 μL, 0.2 mmol) were added. The reaction was stopped after 24 h by exposing to

air. The resulting polymer was precipitated from methanol. The crude polymer was redissolved in CHCl₃, and the catalyst was removed by passing it over an alumina column. The purified product was obtained through repeated precipitation and dried under vacuum (yield: 0.835 g; conversion: 66.3%; DP_{n,calc} = 9.94 ≈ 10).

Synthesis of Block Copolymer PSPMA-*b*-PtBA via Cu(0)-Mediated LRP. The experiment was carried out at [M]:[I]:[C]:[L]:[R] = 50:1:0.25:0.25:0.25. Solvent (DMSO, 4 mL), PSPMA-Br (I, 0.42g, 0.1 mmol), catalyst (C, copper powder, 1.6 mg, 0.025 mmol), and hydrazine hydrate (R, 1.2 μL, 0.025 mmol) were added to a dried flask. The reaction mixture was stirred for 15 min in a 30 ± 0.1 °C water bath after being degassed and full filled with nitrogen. After that, tBA (M, 0.73 mL, 5 mmol) and the ligand (L, Me₆TREN, 6.4 μL, 0.025 mmol) were added to start the polymerization. The reaction was stopped after 24 h by exposing to air. The crude polymer was precipitated from the mixed solvent of methanol and water (v/v, 1:1). The purified product was obtained through repeated precipitation and dried under vacuum (yield: 0.928 g; conversion: 79.3%; DP_{n,calc} = 39.7 ≈ 40).

Hydrolysis of PSPMA-*b*-PtBA. The block copolymer PSPMA₁₀-*b*-PtBA₄₀ was dissolved in dry DCM and followed by adding a 5-fold molar excess of TFA. The solution was stirred at 30 °C for 24 h. The hydrolyzate (PSPMA₁₀-*b*-PAA₄₀) was obtained by precipitating in petroleum ether (60–90 °C) and dried under vacuum.

Preparation of Copolymers Aggregates. 1 mg of copolymer was dissolved in 1 mL of DMSO and followed by the dropwise addition of 10 mL of H₂O under vigorous stirring. Then DMSO was completely removed by dialysis against water, and thus the concentration of polymer solution was 0.1 mg/mL. The solution was filtered through a 0.22 μm filter before use.

Light Sources. The UV light source was obtained from a high-pressure mercury lamp equipped with a band-pass filter to get an emission wavelength at 365 nm. The intensity of the UV light was 3 mW cm⁻². The source of visible light (620 nm) was a tungsten 40 W lamp that generated a power of 2 mW cm⁻². The samples were placed at a distance of 5 cm from the light source in quartz cuvettes at room temperature.

Measurements. ¹H NMR Spectroscopy. The compositions of copolymers were determined by nuclear magnetic resonance (¹H NMR) spectroscopy (Varian Mercury plus 400, 400 MHz) in CDCl₃ or DMSO-*d*₆ with tetramethylsilane (TMS) internal standard.

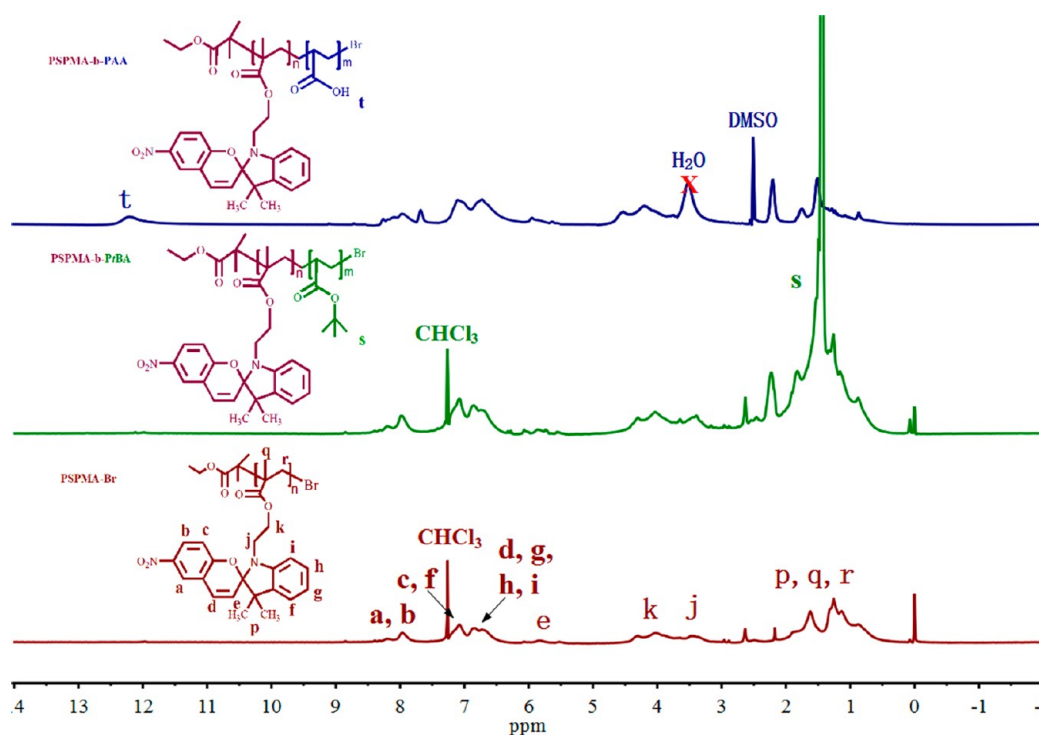


Figure 1. ^1H NMR spectra of $\text{PSPMA}_{10}\text{-}b\text{-PAA}_{40}$ (in blue, top), $\text{PSPMA}_{10}\text{-}b\text{-PtBA}_{40}$ (in green, middle), and $\text{PSPMA}_{10}\text{-Br}$ (in dark red, bottom).

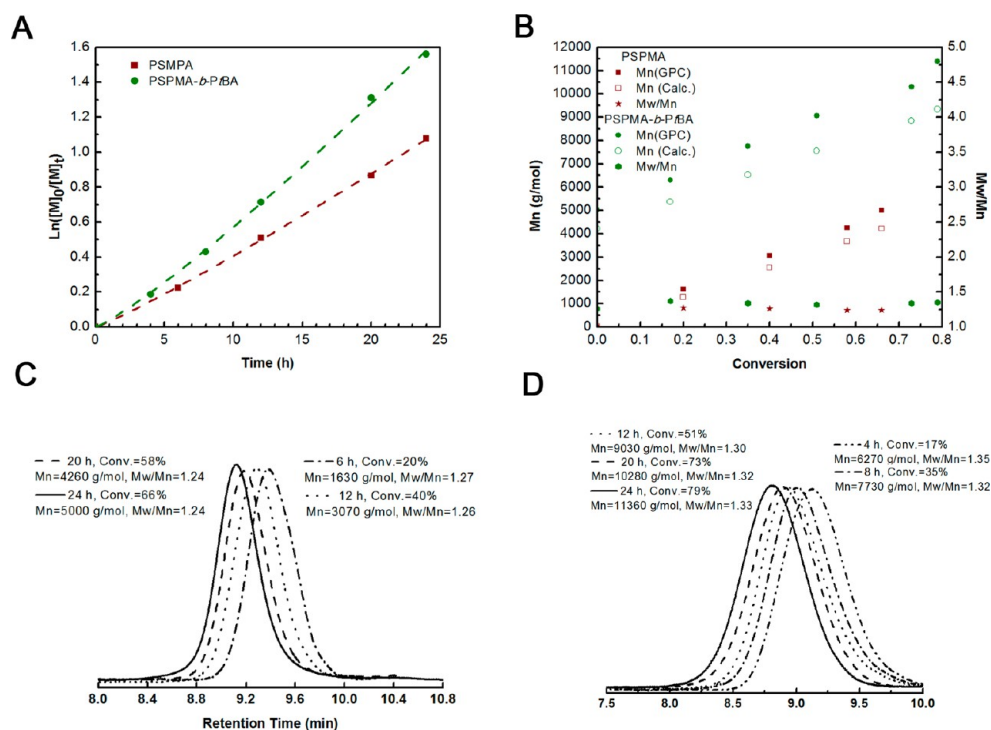


Figure 2. Kinetic plot for the synthesis of PSPMA-Br and $\text{PSPMA-}b\text{-PtBA}$ (A); evolution of M_n and M_w/M_n (B); GPC traces with monomer conversion for the synthesis of PSPMA-Br (C); and GPC traces with monomer conversion for the synthesis of $\text{PSPMA-}b\text{-PtBA}$ (D).

Gel Permeation Chromatography (GPC). Molecular weights and molecular weight distributions (M_w/M_n) of polymer were determined on a gel permeation chromatograph (GPC, Tosoh Corporation) equipped with two HLC-8320 columns (TSK gel Super AWM-H, pore size: $9\ \mu\text{m}$; $6 \times 150\ \text{mm}$, Tosoh Corporation) and a double-path, double-flow a refractive index detector (Bryce) at $30\ ^\circ\text{C}$. The elution phase was DMF (0.01 mol/L LiBr, elution rate: 0.6 mL/min), and a

series of poly(methyl methacrylate) (PMMA) were used as the calibration standard.

Transmission Electron Microscopy (TEM). The TEM images of self-assembly samples were obtained using a JEM-2100 (JEOL Ltd., Japan) transmission electron microscope operated at an acceleration voltage of 200 kV. The samples were prepared by dropping the solution of onto copper grids coated with a thin carbon film and then dried at $25\ ^\circ\text{C}$ for 48 h. No staining treatment was performed for the measurement.

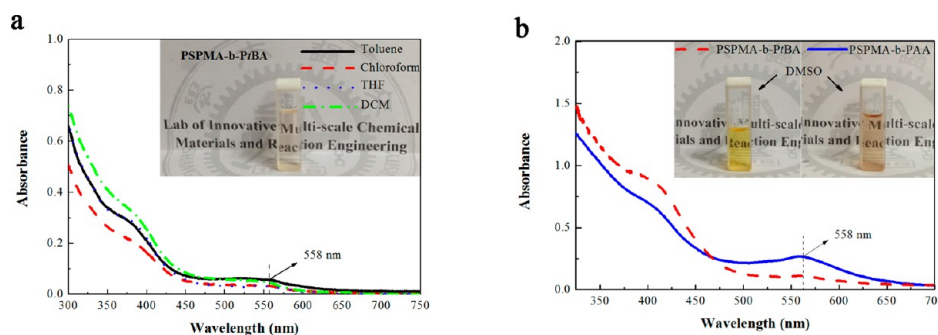


Figure 3. UV–vis spectra of the PSPMA₁₀-*b*-PtBA₄₀ copolymers in solvents with different polarity (0.1 mg/mL) (a); the comparison of PSPMA₁₀-*b*-PAA₄₀ and PSPMA₁₀-*b*-PtBA₄₀ in DMSO (0.2 mg/mL) (b). The insets represent the photograph of copolymer solutions before UV irradiation.

Dynamic Light Scattering (DLS). DLS measurements were performed on the self-assembly aqueous solutions using a ZS90 Zetasizer Nano ZS instrument (Malvern Instruments Ltd., U.K.) equipped with a 4 mW He–Ne laser ($\lambda = 633$ nm) at an angle of 90° . Zeta potential studies of self-assembly aqueous solutions were determined at various pH. No background electrolyte was added. The reported data were measured for three runs.

UV–vis Spectra. The UV–vis spectra were obtained via UV-2550 spectrophotometer (Shimadzu, Japan). The solutions were equilibrated for 10 min before measurement, and the concentration of the polymer solution is 0.1 or 0.2 mg/mL.

RESULTS AND DISCUSSION

Synthesis of the Block Copolymer by Cu(0)-Mediated LRP. Cu(0)-mediated LRP was chosen to produce PSPMA₁₀-*b*-PtBA₄₀ due to the low-temperature polymerization condition, minor amount of catalyst, suitability for acrylic monomer, and perfect end-functionality.^{47–52} Reducing agent (i.e., hydrazine hydrate) was added into the reaction system in order to ensure the anaerobic experimental condition and eliminate the time-consuming deoxygenating cycles needed before polymerization. During the experiments, an equimolar amount of reducing agent hydrazine hydrate (with respect to Cu(0)) was employed. Therefore, the copper was activated as the Cu₂O located on the surface of copper powder was reduced to Cu(0), which acted an effective oxygen scavenger in reagents before polymerization.⁵² In addition, if there was excess reducing agent, it would efficiently reduce the Cu(II) complexes presented in the system to the corresponding Cu(I) complexes as has been well-documented by Matyjaszewski et al.⁵³

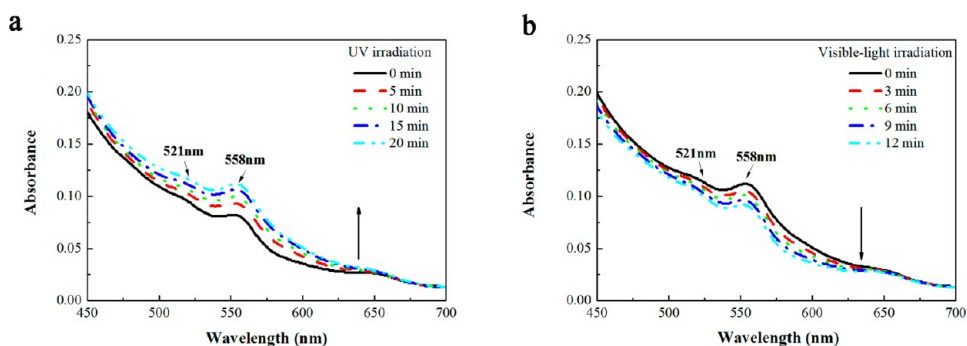
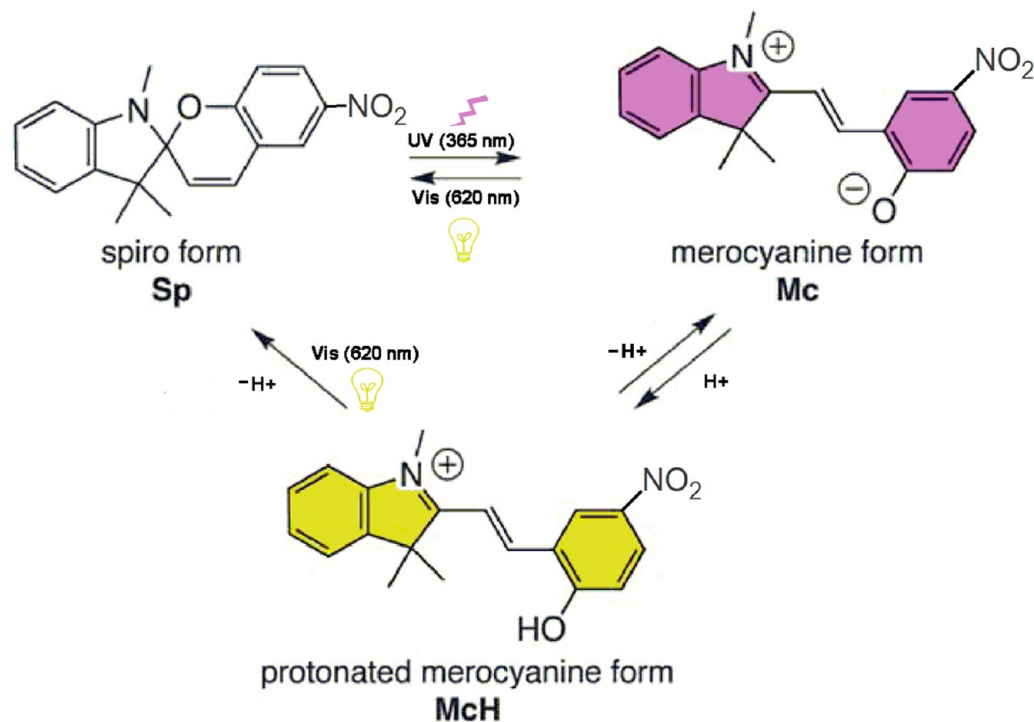
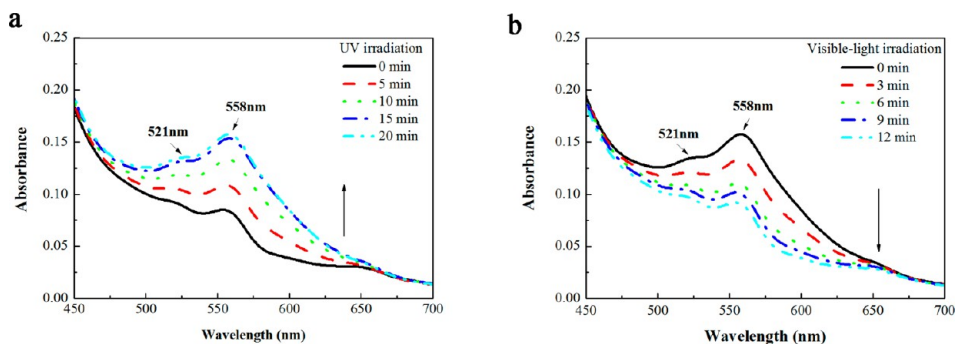
As depicted in Scheme 1, the macroinitiator PSPMA₁₀-Br was synthesized via Cu(0)-mediated LRP at 30 °C. The number of subscript represents the average degree of polymerization (DP_n) of macroinitiator, which is obtained from monomer conversion and verified by comparing the characteristic peak area for the proton of the benzopyran phenyl group near the nitro (8.01–8.03 ppm, 2H, ArH) and the methylene protons of the initiator (4.10 ppm, 2H, $-\text{OCH}_2\text{CH}_3$). The resultant polymer characterized by ¹H NMR is shown in Figure 1 (bottom). The theoretical DP_n calculated by ¹H NMR is approximately 10, namely $M_n = 4201$ g/mol, which agrees with the GPC result (5000 g/mol) within allowable error. Additionally, the characteristic peak area ratio of PtBA indicates that the DP_n of PtBA block is approximately 40 [(1.35–1.55 ppm, 9H, $-\text{OC}(\text{CH}_3)_3$) and PSPMA (8.01–8.03 ppm, 2H, ArH) (Figure 1, middle)]. The M_n of block copolymer (PSPMA₁₀-*b*-PtBA₄₀) obtained from the chain extension of macroinitiator PSPMA₁₀-Br is 9328 g/mol by theory and 11360 g/mol by GPC measurement.

Figure 2A shows the kinetic plot for the synthesis of PSPMA₁₀ and PSPMA₁₀-*b*-PtBA₄₀ by Cu(0)-mediated LRP. It illustrated that both polymerization processes followed pseudo-first-order kinetics with slightly increasing propagation rate after 5 h, which indicates the complete reduction of Cu₂O. A linear increase in M_n with the conversion for both polymers shows a typical successful Cu(0)-mediated LRP under such oxygen-tolerant system⁵¹ as displayed in Figure 2B. The relatively broader M_w/M_n (1.24 for PSPMA, 1.33 for PSPMA-*b*-PtBA) may result from the irreversible termination favored by highly reactive Cu(0) powder with an increasing radical concentration and decreasing deactivator concentration caused by the reduction of Cu(II) by an excess of hydrazine.⁵¹ However, the value of M_w/M_n is smaller than 1.5, proving that the polymerization is still under control. The M_n obtained by GPC test deviates from theoretical calculation during the reaction, which can be ascribed to the difference between the resulting polymers and narrow PMMA standards. Figures 2C,D demonstrate that the retention time in GPC for both resulting polymers decrease monodirectionally with increasing reaction time, indicating the increment of molecular weight. The GPC traces for the synthesis of block copolymer show slight tailing toward low molecular weight, which can be attributed to the inefficient initiation and formation of dead chains. Despite above-mentioned minor defects, the polymerization mediated by Cu(0) features quasi-living and controllable characteristic.

From ¹H NMR (Figure 1, top) result, one can find that the signal of the *tert*-butyl at 1.45 ppm disappears, whereas the peak at 12.30 ppm attributed to the protons of carboxyl groups appears. Therefore, the DHBC PSPMA₁₀-*b*-PAA₄₀ was obtained via hydrolysis of PSPMA₁₀-*b*-PtBA₄₀ in the presence of TFA.

Solvatochromic Behavior of the Block Copolymers. As well-known, the photochromism of Sp is probably affected by the polarity of surroundings, such as solvent and polymer matrix. Figure 3 shows the UV–vis spectra of PSPMA₁₀-*b*-PtBA₄₀ polymer (0.1 mg/mL) dissolved in five organic solvents, specifically, toluene, chloroform, THF, DCM, and DMSO. These solvents have increasing solvent dipolarity-polarizability (SPP) scales,³⁵ which is 0.655, 0.786, 0.838, 0.876, and 1.000, respectively. One can find that the spiropyran-based copolymer containing nonpolar *t*BA comonomer is not sensitive to the polarity of the surrounding environment, and the light yellow polymer solution was observed (see Figure 3a, inset) for all solvents, as has been previously confirmed.³⁵ The low-intensity absorption band at about 558 nm attributed to the Mc form and a relatively high intensity band at 370–400 nm assigned to nonpolar Mc isomer were observed in all solutions in Figure 3a. The results implied that the nonpolar character of *t*BA

Scheme 2. Light-Induced Isomerizations of Spirobenzopyran Isomers

Figure 4. UV-vis spectra of PSPMA₁₀-*b*-PtBA₄₀ copolymer solution (0.1 mg/mL in DMSO) upon irradiation with UV light (a) and visible light (b).Figure 5. UV-vis spectra of PSPMA₁₀-*b*-PAA₄₀ copolymer solution (0.1 mg/mL in DMSO) upon irradiation with UV light (a) and visible light (b).

comonomer could not stabilize the open Mc form but stabilize the nonpolar photoisomer. Such a phenomenon is known as “normal photochromism”.

On the other hand, the effect of polymer matrix on solvatochromic behavior before UV irradiation was studied based on the different polarities of the resulting copolymers (PSPMA₁₀-*b*-PAA₄₀ and PSPMA₁₀-*b*-PtBA₄₀). For the sake of

enhancing the visual effect, the concentration of copolymer solution (0.2 mg/mL) was doubled than those of four solutions discussed above. Besides, DMSO was chosen due to its good solubility for both copolymers. Apparently, polymer (PSPMA₁₀-*b*-PtBA₄₀) solution appeared gold colored which was attributed to the nonpolar photoisomer, and the low-intensity absorption band at around 558 nm still existed as shown in Figure 3b.

Compared to PSPMA₁₀-*b*-PtBA₄₀, its hydrolysis product PSPMA₁₀-*b*-PAA₄₀ containing -COOH polar groups has a different characteristic absorption spectrum. As shown in Figure 3b, right inset, the solution of the planar zwitterionic Mc form has a pale violet color, and its absorption band at 558 nm was significantly enhanced. The differences between these two copolymers demonstrated that the colored Mc form was stabilized by polar AA comonomer and thus favored the “reverse photochromism”. As a whole, the solvatochromic property of the copolymer influenced by the polarity of comonomer is suitable to produce optical materials or metal ions thin film sensors.³⁵

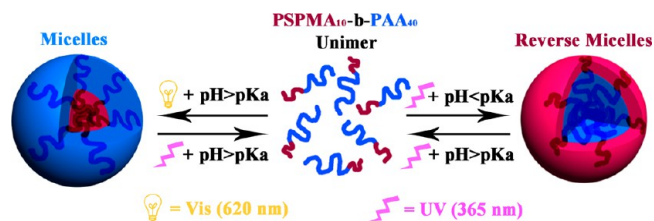
Isomerization Behavior of the Spiropyran Moieties Involved in Block Copolymers. Photochemical isomerization of spiropyran moieties from Sp to Mc is illustrated in Scheme 2 and monitored by UV–vis spectroscopy. The initial solutions of both block copolymers (0.1 mg/mL in DMSO) were irradiated by visible light for 0.5 h to ensure the formation of Sp. Responding to continuous UV irradiation (365 nm; Figures 4a and 5a), a gradual increasing intensity of the absorption band centered at 558 nm indicates the isomerization of Sp to Mc form. On the contrary, the reverse isomerization process from Mc to Sp induced by visible light irradiation was described by the spectra with gradually downward trend (620 nm; Figures 4b and 5b).

After 20 min of UV irradiation and 12 min of visible light irradiation, PSPMA₁₀-*b*-PtBA₄₀ and PSPMA₁₀-*b*-PAA₄₀ copolymer solution systems reached a plateau which implies the achievement of photostationary state. But, there are significant differences between these two copolymers in the absorption intensity. Compared to the spectra with wide range in Figure 3, a hypochromatic shift of absorption band from 558 to 521 nm exists in the enlarged view of spectra (Figures 4 and 5), which is corresponded to H-type Sp-Mc, and intramolecular Mc_n stacks.²⁹ The behaviors of H-type aggregation can be strongly enhanced in a system, which contains high chromophore content and stabilizes the planar zwitterionic Mc isomer.⁵⁵ For this reason, the enhancement of absorption intensity at 521 nm appeared in PSPMA₁₀-*b*-PAA₄₀ system. In addition, the corresponding increase in 558 nm was ascribed to the effect of the polar polymer matrix, which contributes to the Mc form stabilization as discussed above. It is worth noting that the arrival time of photostationary state is affected not only by the polymer system but also by the intensity of UV light or visible light.

“Schizophrenic” Micellization Behavior of PSPMA-*b*-PAA. The spiropyran (Sp) compound is generally insoluble in water, but its hydrophilicity can be enhanced after the photoisomerization process. Meanwhile, the solubility of PAA block in water depends on the pH of aqueous solution. Since the hydrolysis of PSPMA₁₀-*b*-PtBA₄₀ leads to a DHBC PSPMA₁₀-*b*-PAA₄₀, it is expected that spiropyran-based polymer conjugating with pH-responsive water-soluble polymer will exhibit the “schizophrenic” micellization behavior in response to light or pH stimulus in aqueous system. The proposed mechanism is shown in Scheme 3, and the micellar structure is monitored by TEM in Figure 6.

With respect to micellization behavior, the PAA segments readily dissolve in water and form a shell to contact with water because the carboxylate groups involved in PAA blocks start to be deprotonated at pH > pK_a.⁵⁶ On the other hand, the Sp isomer is stable in alkaline media^{35,34} and forms the closely packed core. In theory, micelles with the PSPMA core should be obtained by the application of visible light stimulus and the alkaline aqueous solution. However, TEM image (Figure 6A) shows spherical aggregates with an average diameter of 100 nm in such

Scheme 3. Representation of “Schizophrenic” Micellization Behavior for PSPMA₁₀-*b*-PAA₄₀ in Aqueous System Regulated by Light or pH Stimulus



circumstance (pH = 11.3). Given the contour length of PSPMA chains (10 repeating units) and PAA (40 repeating units) based on a fully stretched copolymer chain, the size of formed aggregates probably suggests that they do not correspond to isolated micelles but to larger compound micelles.^{46,57} Scheme 4 illustrates that the intriguing micellar morphology comprises inverse micelles containing PAA core and PSPMA corona as well as a hydrophilic PAA backbone in the exterior which endows the micelles a relatively stable nature. In addition, DLS was also used to obtain the average-size and size distribution of micelles as shown in Figure 7A. Herein, the larger diameter in DLS results than that from TEM images might cause by the different testing condition as compared in Table 1, where the micellar sizes measured by DLS are with water-swollen corona, while the samples for TEM are nearly dry under high vacuum. The polyelectrolyte effect which artificially increased the micelle size is probably another reason. In addition, the zeta potential of micellar solution is about -43 mV, which indicates the existence of deprotonated carboxylate groups outside the large compound micelles.

The disruption of the large compound micelles occurred in response to UV light irradiation at $\lambda = 365$ nm was observed followed by UV–vis absorption spectroscopy (Figure 8a) as well as TEM images (Figures 6B,C). As mentioned above, the characteristic absorption band of Mc form at 558 nm appeared and the intensity gradually increased as UV irradiation time went on. During this process, the Mc is more stable than McH form due to the alkaline environment. However, there was a hypochromatic shift of the absorption band from 558 to 521 nm in the spectra, corresponding to H-type Sp-Mc, and intramolecular Mc_n stacks. The behavior of H-type aggregation was greatly enhanced compared to the organic solution system, resulting from the micellar system with high chromophore contents within the large compound micellar core. The TEM image in Figure 6B demonstrated the malformed core–corona structure during the disruption process at 10 min, and thus the anomalous and polydisperse result was found in DLS measurement (Figure 7B). After 50 min, the photostationary state was reached, indicating the disruption of the initial micelles. In addition, it can be seen from Figure 6C that the disappearance of the micelles occurred in solution after UV irradiation since only nonstructured polymer with mutual entanglement of macromolecular chains was observed. Meanwhile, the DLS results also confirmed this result in Figure 7C.

The lower the pH of aqueous solution is, the more carboxylate groups are protonated, and thus the solubility of PAA significantly decreases. In acid medium, almost all chromophores existed as the protonated merocyanine form (McH) responding to UV irradiation, and thus reverse micelles with PAA core and PSPMA corona are obtained. In addition, previous studies showed that lower solution pH favors the isomerization of

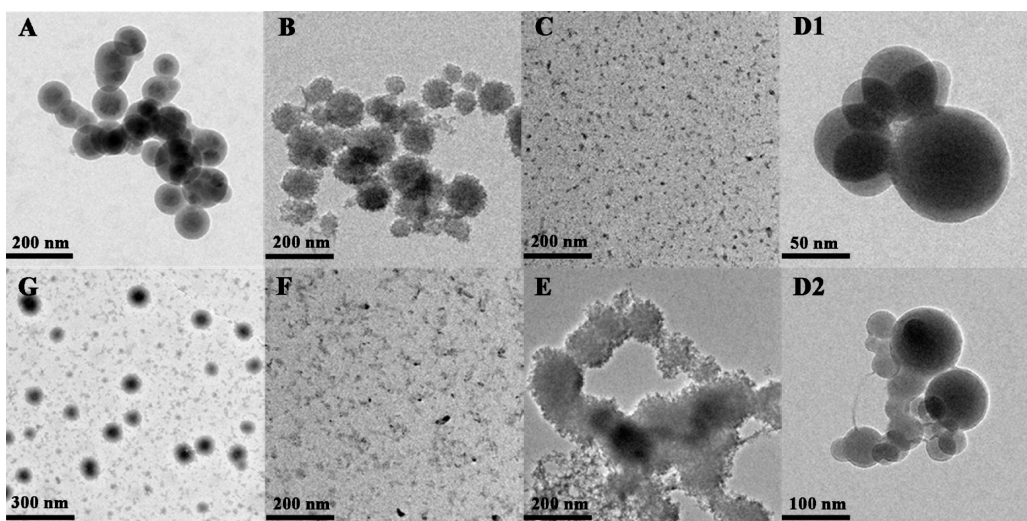


Figure 6. TEM images of micelles at different time about reversible “schizophrenic” micellization behavior investigated in this study (clockwise): (A) micelles with PSPMA core under continuous visible-light irradiation in alkaline aqueous solution (pH = 11.3); (B) the disruption of micelles with PSPMA core after UV irradiation for 10 min; (C) PSPMA₁₀-*b*-PAA₄₀ unimer in aqueous solution at pH = 11.3 after UV irradiation for 50 min; (D1 and D2) reverse micelles with PAA core under continuous UV irradiation at pH = 4.3; (E) the disruption of micelles with PAA core after increasing pH value to 7.5; (F) PSPMA₁₀-*b*-PAA₄₀ unimer in alkaline aqueous solution at pH = 11.3 keeping UV irradiation; (G) reversibly self-assemble into micelles with PSPMA core under continuous visible-light irradiation.

Scheme 4. Representation of the Formation and pH Responsivity of PSPMA-*b*-PAA Large Compound Micelle

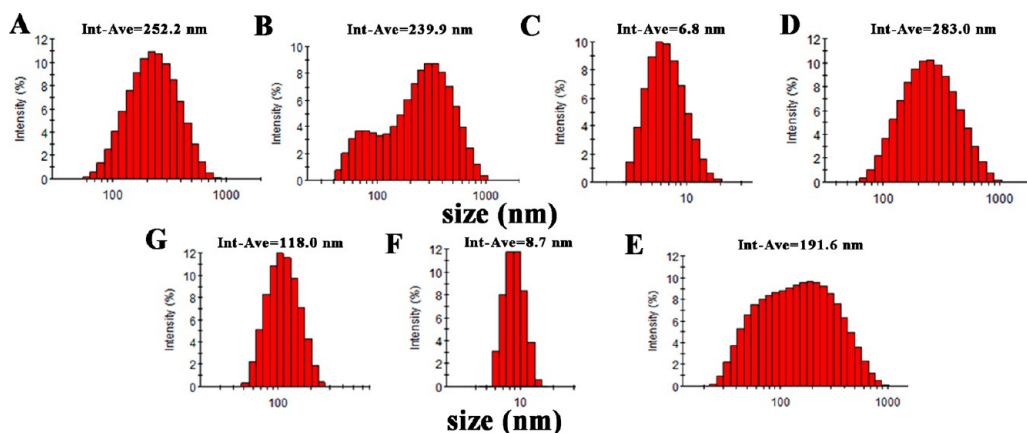
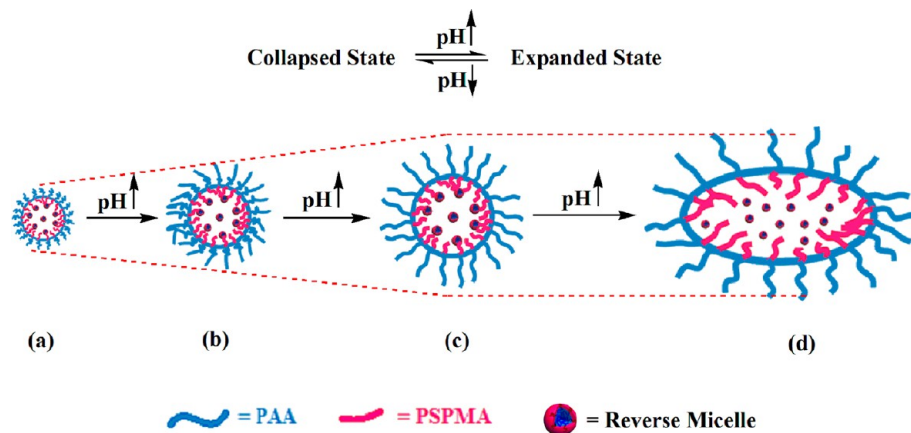


Figure 7. DLS results of micellar solution at different time about reversible “schizophrenic” micellization behavior investigated in this study corresponding to samples in Figure 5 (clockwise).

chromophores from Sp to Mc and leads to the formation of protonated Mc (McH).^{35,54} Similarly, the spherical aggregates

with the diameter about 50–100 nm (Table 1) at pH = 4.3 were demonstrated by TEM images (Figures 6D1,D2), and their

Table 1. Summary of the Micellar Average Diameter and Zeta Potentials Measured by TEM and DLS in Aqueous Solution^a

method	samples						
	A	B	C	D	E	F	G
TEM (nm)	101.2–136.5	NG	~7.6	50.6–102.3	NG	~8.8	70.5–96.2
DLS (Z-av, nm)	181.0	165.1	4.8	203.1	137.5	6.2	84.7
DLS (zeta potential, mV)	-43.1	NG	NG	8.1	NG	NG	-36.7

^aSamples A–G are corresponding to samples in Figure 5 (clockwise); NG = not given.

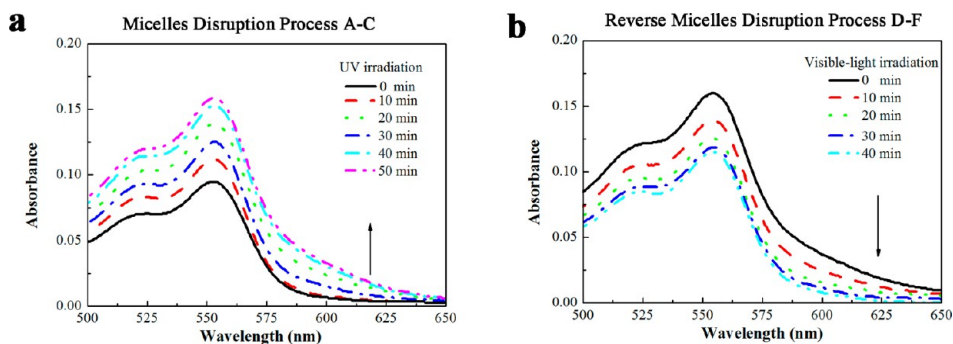


Figure 8. UV-vis spectra of a PSPMA₁₀-*b*-PAA₄₀ micellar system in aqueous solution (0.1 mg/mL) upon irradiation with UV light (a) and visible light (b).

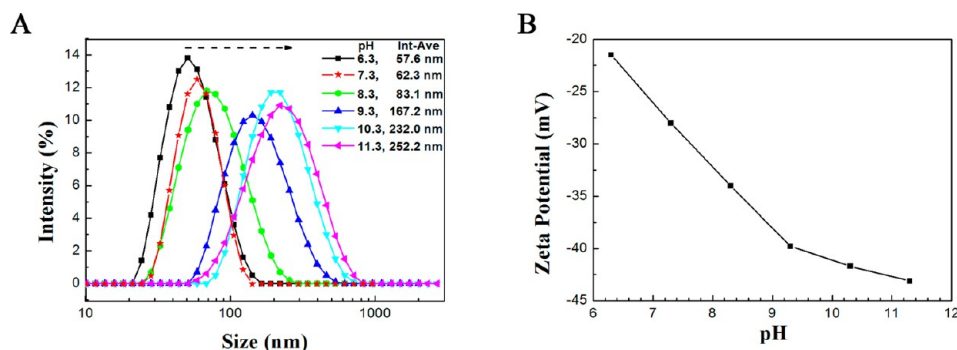


Figure 9. Intensity-averaged sizes (A) and zeta potential (B) of PSPMA₁₀-*b*-PAA₄₀ micellar system measured by DLS in aqueous solution with various pH.

hydrodynamic average size was obtained by DLS result (Figure 7D). Nevertheless, the corona structure was too thin to be observed clearly due to the short PSPMA blocks, and the observed reverse micelles might be also recognized as reverse large compound micelles. On this occasion, some micelles with PSPMA core and PAA corona constitute the core of large compound micelles as well as hydrophilic PSPMA chains dominate the outer surface of large compound micelles. The positively charged micellar solution indicated by zeta potential (8.1 mV) in Table 1 can be accounted by the aggregation of protonated Mc isomer in the corona of reverse large compound micelles.

Reversibly, the rise of pH ($>pK_a$) results in the deprotonation of AA groups, and the large reverse compound micelles will disrupt again, hence molecularly dissolve in aqueous medium. The TEM graph in Figure 6E demonstrated the malformed aggregation again during the disruption process at pH = 7.5, and DLS measurement showed the anomalous and polydisperse result in Figure 7E. The TEM (Figure 6F) and DLS (Figure 7F) results therefore held true for the above discussion of our results in neutral to alkaline aqueous buffer (pH = 11.3), which thus constitutes a good solvent for PSPMA₁₀-*b*-PAA₄₀. Followed by visible light stimuli (620 nm), the micellization was aroused again

with an effective isomerization of the Mc into Sp. The regeneration of micelles was investigated by UV-vis absorption spectroscopy (Figure 8b). The downward trend of spectra verified the isomerization process and implied the aggregation completed within 40 min. The number-average diameters of micelles confirmed by TEM (Figure 6G) and DLS (Figure 7G) were lower than 100 nm as summarized in Table 1. The dispersion of micelles easily found at this time might be explained by the decrease of micellar number and the aggregate chain number per micelle, namely the efficiency of self-assembly decreased as has been previously observed,³⁸ and thus enlarged the distance and decrease of the collision chance between the micelles. Additionally, the lower zeta potential (-36.7 mV) can serve as powerful evidence for the partial regeneration of large compound micelles. As a whole, the above study presented a reversible, light, and pH-induced “schizophrenic” micellization in aqueous system, which is promising for the realization of reversible controlled release of drug.

pH Responsivity of PSPMA-*b*-PAA Large Compound Micelles. In the present study, the formation of micelles implied by TEM and DLS measurements at pH = 11.3 encouraged us to pay more attention to such morphology.

As for the self-assembly of polyelectrolytes, the PAA chains will be ionized at $\text{pH} > \text{pK}_a = 5.5$, and the change of pH will result in the changes of the protonation degree and charge density.^{46,58} From the DLS results in Figure 9A, the micellar size measured at $\text{pH} = 6.3$ is around 60 nm that is unlikely formed by isolated micelles. We suppose that large compound micelles form in the current system, which results from the promptly aggregation of amphiphilic block copolymers with relatively short polymer chains at a high initial concentration of polymer solution as shown in Scheme 4a.^{46,59} On the other hand, the formation of hydrogen bonds between the neighboring micellar shells will postpone the deprotonation of PAA and the dispersion of micelles by the intermicellar attraction.⁴⁵ At higher pH (7.3–11.3), the PAA chains further deprotonate and intramolecular Coulomb repulsion acts as an excluded-volume interaction ensuring the swelling of the polymer micelles via straightening PAA chains and weakening strength of hydrogen bonds.

As a whole, the int-average hydrodynamic radius of micelles increases from 58 to 252 nm with the increase of pH from 6.3 to 11.3, indicating the enlargement of the average number of aggregation (N_{agg}). In order to reduce the entropic penalty resulting from the increasing in stretching degree of PSPMA hydrophobic segments, the large compound micelles first experience the chain expansion ($\text{pH} = 6.3\text{--}9.3$) and followed by the transformation of morphology ($\text{pH} = 9.3\text{--}11.3$), leading to a change in dimension of micelles as illustrated in Scheme 4b–d.

Furthermore, one can observe from Figure 9B increasing pH ionizes carboxylic acid and converts PAA to polyelectrolyte, which gave rise to the downtrend of zeta potential from -21.5 to -43.1 mV. The zeta potential of the micelles decreased rapidly at $\text{pH} < 9.3$, while it only changes slightly when pH is further increased. The slow increase of zeta potential at the pH above 9.3 was also confirmed the formation of stable micelles. This variation trend agrees well with the DLS result. Both the above results confirm that the micelles exhibit a pH-induced dimensional change due to the progressively deprotonating of the PAA chains with the increase of pH and the electrostatic repulsion of the carboxylic anions forces the chains to unbend as well as the transformation of micellar morphology induced by three forces (the core chain stretching, corona chain repulsion, and interfacial tension).⁶⁰

CONCLUSION

In this work, we have successfully synthesized the “schizophrenic” block copolymer, $\text{PSPMA}_{10}\text{-}b\text{-PAA}_{40}$, via sequential Cu(0)-mediated LRP at 30 °C in an oxygen-tolerant system (all reagents without deoxygenating) and hydrolysis reaction.

With respect to solvatochromic behavior, the polarity of the surrounding solvent environment has little influence on the spiropyran-based copolymer containing nonpolar *t*BA comonomer. However, the polar AA comonomer involved in $\text{PSPMA}_{10}\text{-}b\text{-PAA}_{40}$ copolymers stabilizes the planar zwitterionic colored Mc form, while the nonpolar *t*BA stabilizes the nonpolar photoisomer and therefore favors the “reverse” and “normal” photochromism, respectively. Additionally, the upward and downward trend of the UV–vis absorption spectra illustrated the photochemical isomerization of spiropyran moieties induced by UV light and visible light irradiation.

Finally, the expected “schizophrenic” micellization behavior in aqueous media regulated by light and pH stimuli was vividly demonstrated. The TEM and DLS results confirmed polymeric micelles reversible formed in an aqueous solution: normal large

compound micelles form in alkaline aqueous solution under visible light irradiation and disrupt in response to UV irradiation; reverse large compound micelles generate by reducing the value of pH until below pK_a ; normal large compound micelles regenerate by rising pH until higher than pK_a and irradiation with visible light. Notably, normal large compound micelles can bring out a gradually extended conformation in a broad pH range due to the increase of the deprotonation degree and charge density.

Our present dual-stimuli responsive system is worth exploring for environmental and biological application in the future, for instance, the release of hydrophobic molecules in water and applied as metal ions thin film sensors.

ASSOCIATED CONTENT

Supporting Information

Experimental part for the synthesis of spiropyran monomer. This material is available free of charge via the Internet at <http://pubs.acs.org>.

AUTHOR INFORMATION

Corresponding Author

*E-mail luozh@sjtu.edu.cn; Tel +86-21-54745602; Fax +86-21-54745602 (Z.-H.L.).

Notes

The authors declare no competing financial interest.

ACKNOWLEDGMENTS

The authors thank the National Natural Science Foundation of China (No. 21276213, 21076171), the State Key Laboratory of Coal Conversion of China (No. J13-14-102), and the Key Laboratory of Advanced Control and Optimization for Chemical Processes of the National Ministry of Education of China (No. 2012ACOC03) for supporting this work. The authors thank Dr. Xuesong Jiang and Dr. Jianhua Fang (School of Chemistry and Chemical Engineering, Shanghai Jiao Tong University) for their kind suggestions and meaningful contribution to the manuscript.

REFERENCES

- (1) Klaiherd, A.; Nagamani, C.; Thayumanavan, S. Multi-Stimuli Sensitive Amphiphilic Block Copolymer Assemblies. *J. Am. Chem. Soc.* **2009**, *131*, 4830–4838.
- (2) Stuart, M. A. C.; Huck, W. T. S.; Genzer, J.; Müller, M.; Ober, C.; Stamm, M.; Sukhorukov, G. B.; Szleifer, I.; Tsukruk, V. V.; Urban, M.; Winnik, F. M.; Zauscher, S.; Luzinov, I.; Minko, S. Emerging Applications of Stimuli-Responsive Polymer Materials. *Nat. Mater.* **2010**, *9*, 101–113.
- (3) Liu, F.; Urban, M. W. Recent Advances and Challenges in Designing Stimuli-Responsive Polymers. *Prog. Polym. Sci.* **2010**, *35*, 3–23.
- (4) Roy, D.; Cambre, J. N.; Sumerlin, B. S. Future Perspectives and Recent Advances in Stimuli-Responsive Materials. *Prog. Polym. Sci.* **2010**, *35*, 278–301.
- (5) Liu, S.; Armes, S. P. Synthesis and Aqueous Solution Behavior of a pH-Responsive Schizophrenic Diblock Copolymer. *Langmuir* **2003**, *19*, 4432–4438.
- (6) Gu, L.; Feng, C.; Yang, D.; Li, Y.; Hu, J.; Lu, G.; Huang, X. PEGMEA-g-PDEAEMA: Double Hydrophilic Double-grafted Copolymer Stimuli-Responsive to Both pH and Salinity. *J. Polym. Sci., Part A: Polym. Chem.* **2009**, *47*, 3142–3153.
- (7) Jiang, X.; Zhang, G.; Narain, R.; Liu, S. Fabrication of Two Types of Shell-Cross-Linked Micelles with “Inverted” Structures in Aqueous

Solution from Schizophrenic Water-Soluble ABC Triblock Copolymer via Click Chemistry. *Langmuir* **2009**, *25*, 2046–2054.

(8) Smith, A. E.; Xu, X.; Kirkland-York, S. E.; Savin, D. A.; McCormick, C. L. Schizophrenic Self-Assembly of Block Copolymers Synthesized via Aqueous RAFT Polymerization: From Micelles to Vesicles. *Macromolecules* **2010**, *43*, 1210–1217.

(9) Zhai, S.; Song, X.; Yang, D.; Chen, W.; Hu, J.; Lu, G.; Huang, X. Synthesis of Well-Defined pH-Responsive PPEGMEA-g-P2VP Double Hydrophilic Graft Copolymer via Sequential SET-LRP and ATRP. *J. Polym. Sci., Part A: Polym. Chem.* **2011**, *49*, 4055–4064.

(10) Feng, C.; Li, Y.; Yang, D.; Li, Y.; Hu, J.; Zhai, S.; Lu, G.; Huang, X. Synthesis of Well-Defined PNIPAM-b-(PEA-g-P2VP) Double Hydrophilic Graft Copolymer via Sequential SET-LRP and ATRP and its “Schizophrenic” Micellization Behavior in Aqueous Media. *J. Polym. Sci., Part A: Polym. Chem.* **2010**, *48*, 15–23.

(11) Arotçaréna, M.; Heise, B.; Ishaya, S.; Laschewsky, A. Switching the Inside and the Outside of Aggregates of Water-Soluble Block Copolymers with Double Thermoresponsivity. *J. Am. Chem. Soc.* **2002**, *124*, 3787–3793.

(12) Jin, Q.; Liu, G.; Ji, J. Micelles and Reverse Micelles with A Photo and Thermo Double-Responsive Block Copolymer. *J. Polym. Sci., Part A: Polym. Chem.* **2010**, *48*, 2855–2861.

(13) Zhai, S.; Wang, B.; Feng, C.; Li, Y.; Yang, D.; Hu, J.; Lu, G.; Huang, X. Thermoresponsive PPEGMEA-g-PPEGEMA Well-Defined Double Hydrophilic Graft Copolymer Synthesized by Successive SET-LRP and ATRP. *J. Polym. Sci., Part A: Polym. Chem.* **2010**, *48*, 647–655.

(14) Guragain, S.; Bastakoti, B. P.; Yusa, S. I.; Nakashima, K. Stimuli-Induced Core-Corona Inversion of Micelles of Water-Soluble Poly-(sodium 2-(acrylamido)-2-methyl propanesulfonate-*b*-*N*-isopropylacrylamide). *Polymer* **2010**, *51*, 3181–3186.

(15) Bertrand, O.; Fustin, C. A.; Gohy, J. F. Multiresponsive Micellar Systems from Photocleavable Block Copolymers. *ACS Macro Lett.* **2012**, *1*, 949–953.

(16) Zhao, Y. Light-Responsive Block Copolymer Micelles. *Macromolecules* **2012**, *45*, 3647–3657.

(17) Dai, S.; Ravi, P.; Tam, K. C. Thermo- and Photo-Responsive Polymeric Systems. *Soft Matter* **2009**, *5*, 2513–2533.

(18) Butun, V.; Billingham, N. C.; Armes, S. P. Unusual Aggregation Behavior of a Novel Tertiary Amine Methacrylate-Based Diblock Copolymer: Formation of Micelles and Reverse Micelles in Aqueous Solution. *J. Am. Chem. Soc.* **1998**, *120*, 11818–11819.

(19) Butun, V.; Liu, S.; Weaver, J. V. M.; Bories-Azeau, X.; Cai, Y.; Armes, S. P. A Brief Review of ‘Schizophrenic’ Block Copolymers. *React. Funct. Polym.* **2006**, *66*, 157–165.

(20) Tyrrell, Z. L.; Shen, Y.; Radosz, M. Fabrication of Micellar Nanoparticles for Drug Delivery through the Self-assembly of Block Copolymers. *Prog. Polym. Sci.* **2010**, *35*, 1128–1143.

(21) Feng, C.; Li, Y.; Yang, D.; Hu, J.; Zhang, X.; Huang, X. Well-Defined Graft Copolymers: From Controlled Synthesis to Multipurpose Applications. *Chem. Soc. Rev.* **2011**, *40*, 1282–1295.

(22) Ge, Z.; Liu, S. Functional Block Copolymer Assemblies Responsive to Tumor and Intracellular Microenvironments for Site-Specific Drug Delivery and Enhanced Imaging Performance. *Chem. Soc. Rev.* **2013**, *42*, 7289–7325.

(23) Feng, C.; Shen, Z.; Li, Y.; Gu, L.; Zhang, Y.; Lu, G.; Huang, X. PNIPAM-*b*-(PEA-g-PDMAEA) Double-Hydrophilic Graft Copolymer: Synthesis and Its Application for Preparation of Gold Nanoparticles in Aqueous Media. *J. Polym. Sci., Part A: Polym. Chem.* **2009**, *47*, 1811–1824.

(24) Gaitzsch, J.; Appelhans, D.; Wang, L. G.; Battaglia, G.; Voit, B. Synthetic Bio-Nanoreactor: Mechanical and Chemical Control of Polymersome Membrane Permeability. *Angew. Chem., Int. Ed.* **2012**, *51*, 4448–4451.

(25) Lu, A.; O’Reilly, R. K. Advances in Nanoreactor Technology Using Polymeric Nanostructures. *Curr. Opin. Biotechnol.* **2013**, *24*, 639–645.

(26) Wu, Y.; Hu, H.; Hu, J.; Liu, T.; Zhang, G.; Liu, S. Thermo- and Light-Regulated Formation and Disintegration of Double Hydrophilic

Block Copolymer Assemblies with Tunable Fluorescence Emissions. *Langmuir* **2013**, *29*, 3711–3720.

(27) Pasparakis, G.; Manouras, T.; Argitis, P.; Vamvakaki, M. Photodegradable Polymers for Biotechnological Applications. *Macromol. Rapid Commun.* **2012**, *33*, 183–198.

(28) Jiang, J.; Tong, X.; Zhao, Y. A New Design for Light-Breakable Polymer Micelles. *J. Am. Chem. Soc.* **2005**, *127*, 8290–8291.

(29) Berkovic, G.; Krongauz, V.; Weiss, V. Spiropyran and Spirooxazines for Memories and Switches. *Chem. Rev.* **2000**, *100*, 1741–1753.

(30) Pasparakis, G.; Vamvakaki, M. Multiresponsive Polymers: Nano-Sized Assemblies, Stimuli-Sensitive Gels and Smart Surfaces. *Polym. Chem.* **2011**, *2*, 1234–1248.

(31) Kameda, M.; Sumaru, K.; Kanamori, T.; Shinbo, T. Probing the Dielectric Environment Surrounding Poly(*N*-isopropylacrylamide) in Aqueous Solution with Covalently Attached Spirobenzopyran. *Langmuir* **2004**, *20*, 9315–9319.

(32) Satoh, T.; Sumaru, K.; Takagi, T.; Kanamori, T. Fast-Reversible Light-Driven Hydrogels Consisting of Spirobenzopyran-Functionalized Poly(*N*-isopropylacrylamide). *Soft Matter* **2011**, *7*, 8030–8034.

(33) Piech, M.; Bell, N. S. Controlled Synthesis of Photochromic Polymer Brushes by Atom Transfer Radical Polymerization. *Macromolecules* **2006**, *39*, 915–922.

(34) Tong, R.; Hemmati, H. D.; Langer, R.; Kohane, D. S. Photoswitchable Nanoparticles for Triggered Tissue Penetration and Drug Delivery. *J. Am. Chem. Soc.* **2012**, *134*, 8848–8855.

(35) Achilleos, D. S.; Vamvakaki, M. Multiresponsive Spiropyran-Based Copolymers Synthesized by Atom Transfer Radical Polymerization. *Macromolecules* **2010**, *43*, 7073–7081.

(36) Achilleos, D. S.; Alan Hatton, T.; Vamvakaki, M. Light-Regulated Supramolecular Engineering of Polymeric Nanocapsules. *J. Am. Chem. Soc.* **2012**, *134*, 5726–5729.

(37) Joseph, G.; Pichardo, J.; Chen, G. Reversible Photo-/Thermoresponsive Structured Polymer Surfaces Modified with a Spirobenzopyran-Containing Copolymer for Tunable Wettability. *Analyst* **2010**, *135*, 2303–2308.

(38) Lee, H.; Wu, W.; Oh, J. K.; Mueller, L.; Sherwood, G.; Peteanu, L.; Kowalewski, T.; Matyjaszewski, K. Light-Induced Reversible Formation of Polymeric Micelles. *Angew. Chem., Int. Ed.* **2007**, *46*, 2453–2457.

(39) Wang, Y.; Hong, C. Y.; Pan, C. Y. Spiropyran-Based Hyperbranched Star Copolymer: Synthesis, Phototropy, FRET, and Bioapplication. *Biomacromolecules* **2012**, *13*, 2585–2593.

(40) Oh, Y. J.; Nam, J. A.; Al-Nahain, A.; Lee, S.; In, I.; Park, S. Y. Spiropyran-Conjugated Pluronic as a Dual Responsive Colorimetric Detector. *Macromol. Rapid Commun.* **2012**, *33*, 1958–1963.

(41) Fries, K.; Samanta, S.; Orski, S.; Locklin, J. Reversible Colorimetric Ion Sensors Based on Surface Initiated Polymerization of Photochromic Polymers. *Chem. Commun.* **2008**, *47*, 6288–6290.

(42) Fries, K. H.; Driskell, J. D.; Sheppard, G. R.; Locklin, J. Fabrication of Spiropyran-Containing Thin Film Sensors Used for the Simultaneous Identification of Multiple Metal Ions. *Langmuir* **2011**, *27*, 12253–12260.

(43) Ventura, C.; Byrne, R.; Audouin, F.; Heise, A. Atom Transfer Radical Polymerization Synthesis and Photoresponsive Solution Behavior of Spiropyran End-Functionalized Polymers as Simplistic Molecular Probes. *J. Polym. Sci., Part A: Polym. Chem.* **2011**, *49*, 3455–3463.

(44) Zhao, Y.; Luo, Y. W.; Li, B. G.; Zhu, S. P. pH Responsivity and Micelle Formation of Gradient Copolymers of Methacrylic Acid and Methyl Methacrylate in Aqueous Solution. *Langmuir* **2011**, *27*, 11306–11315.

(45) Li, J. J.; Zhou, Y. N.; Luo, Z. H. Synthesis and pH-Responsive Micellization of Brush Copolymers Poly(methyl methacrylate-*co*-2-(2-bromoisobutyryloxy)ethyl methacrylate-*graft*-acrylic acid): Role of Composition Profile. *Soft Matter* **2012**, *8*, 11051–11061.

(46) Jiang, X.; Lu, G.; Feng, C.; Li, Y.; Huang, X. Poly(acrylic acid)-*graft*-Poly(*N*-vinylcaprolactam): A Novel pH and Thermo Dual-Stimuli Responsive System. *Polym. Chem.* **2013**, *4*, 3876–3884.

(47) Percec, V.; Guliashvili, T.; Ladislaw, J. S.; Wistrand, A.; Stjern Dahl, A.; Sienkowska, M. J.; Monteiro, M. J.; Sahoo, S. Ultrafast Synthesis of Ultrahigh Molar Mass Polymers by Metal-Catalyzed Living Radical Polymerization of Acrylates, Methacrylates, and Vinyl Chloride Mediated by SET at 25 °C. *J. Am. Chem. Soc.* **2006**, *128*, 14156–14165.

(48) Rosen, B. M.; Percec, V. Single-Electron Transfer and Single-Electron Transfer Degenerative Chain Transfer Living Radical Polymerization. *Chem. Rev.* **2009**, *109*, 5069–5119.

(49) Zhang, Y. Z.; Wang, Y.; Peng, C. H.; Zhong, M. J.; Zhu, W. P.; Konkolewicz, D.; Matyjaszewski, K. Copper-Mediated CRP of Methyl Acrylate in the Presence of Metallic Copper: Effect of Ligand Structure on Reaction Kinetics. *Macromolecules* **2012**, *45*, 78–86.

(50) Konkolewicz, D.; Wang, Y.; Zhong, M.; Krys, P.; Isse, A. A.; Gennaro, A.; Matyjaszewski, K. Reversible-Deactivation Radical Polymerization in the Presence of Metallic Copper. A Critical Assessment of the SARA ATRP and SET-LRP Mechanisms. *Macromolecules* **2013**, *46*, 8749–8772.

(51) Zhou, Y. N.; Luo, Z. H. Facile Synthesis of Gradient Copolymers via Semi-Batch Copper(0)-Mediated Living Radical Copolymerization at Ambient Temperature. *Polym. Chem.* **2013**, *4*, 76–84.

(52) Fleischmann, S.; Rosen, B. M.; Percec, V. SET-LRP of Acrylates in Air. *J. Polym. Sci., Part A: Polym. Chem.* **2010**, *48*, 1190–1196.

(53) Matyjaszewski, K.; Jakubowski, W.; Min, K.; Tang, W.; Huang, J.; Braunecker, W. A.; Tsarevsky, N. V. Diminishing Catalyst Concentration in Atom Transfer Radical Polymerization with Reducing Agents. *Proc. Natl. Acad. Sci. U. S. A.* **2006**, *103*, 15309–15314.

(54) Raymo, F. M.; Giordani, S. Signal Processing at the Molecular Level. *J. Am. Chem. Soc.* **2001**, *123*, 4651–4652.

(55) Eckhardt, H.; Bose, A.; Krongauz, V. Formation of Molecular H- and J-Stacks by the Spiropyran-Merocyanine Transformation in A Polymer Matrix. *Polymer* **1987**, *28*, 1959–1964.

(56) Schilli, C. M.; Zhang, M. F.; Rizzardo, E.; Thang, S. H.; Chong, Y. K.; Edwards, K.; Karlsson, G.; Muller, A. H. E. A New Double-Responsive Block Copolymer Synthesized via RAFT Polymerization: Poly(*N*-isopropylacrylamide)-*block*-poly(acrylic acid). *Macromolecules* **2004**, *37*, 7861–7866.

(57) Zhang, L.; Eisenberg, A. Multiple Morphologies and Characteristics of “Crew-Cut” Micelle-like Aggregates of Polystyrene-*b*-poly(acrylic acid) Diblock Copolymers in Aqueous Solutions. *J. Am. Chem. Soc.* **1996**, *118*, 3168–3181.

(58) Sonnenberg, L.; Parvole, J.; Borisov, O.; Billon, L.; Gaub, H. E.; Seitz, M. AFM-Based Single Molecule Force Spectroscopy of End-Grafted Poly(acrylic acid) Monolayers. *Macromolecules* **2006**, *39*, 281–288.

(59) Feng, C.; Lu, G.; Li, Y.; Huang, X. Self-Assembly of Amphiphilic Homopolymers Bearing Ferrocene and Carboxyl Functionalities: Effect of Polymer Concentration, β -Cyclodextrin, and Length of Alkyl Linker. *Langmuir* **2013**, *29*, 10922–10931.

(60) Zhang, L.; Eisenberg, A. Morphogenic Effect of Added Ions on Crew-Cut Aggregates of Polystyrene-*b*-poly(acrylic acid) Block Copolymers in Solutions. *Macromolecules* **1996**, *29*, 8805–8815.